Electronic Supplementary Material (ESI) for Molecular BioSystems


# Bistability in a model of early B cell receptor activation and its role in tonic signaling and system tunability

## SUPPLEMENTARY MATERIAL

### List of contents

# 1. List of ODEs

The model consists of 12 molecular species formed by three proteins including the intermediate complexes. The model has three constraint equations for the total amount of each protein and has nine independent differential equations. The ODEs and the corresponding abbreviations used are listed below. The terms on the right hand side of the the ODEs arise upon using mass action kinetics for the reactions given in the next section of the Supplementary Material. SBML files for the models will be available upon request.

### Abbreviations of the notations used

1. Bm - BCR monomer
2. Bd - BCR dimer
3. L - Free Lyn
4. pL - Phosphorylated Lyn
5. BL – BCR dimer-Lyn complex
6. BpL - BCR-phosphorylated Lyn complex
7. pBL - phosphorylated BCR dimer-Lyn complex
8. pBpL - phosphorylated BCR dimer-phosphorylated Lyn complex
9. ppBL - Doubly phosphorylated BCR dimer-Lyn complex
10. ppBpL - Doubly phosphorylated BCR dimer-phosphorylated Lyn complex
11. SHPi - Inactive SHP
12. SHP - Active SHP

## Model Constraint Equations

1. $BM = Bt - 2\,(Bd + BL + BpL + pBL + pBpL + ppBL + ppBpL)$
2. $L = Lt - (pL + BL + BpL + pBL + pBpL + ppBL + ppBpL)$
3. $SHPi = St - SHP$

## Model ODEs

1. $\frac{d}{dt}Bd = (a_1 + a_2)BM\ BM - d\ Bd - r_1\ Bd\ (L + pL) + dl_0\ (BL + BpL) + dl_1\ (pBL + pBpL) + dl_2\ (ppBL + ppBpL)$
2. $\frac{d}{dt}pL = -r_1\ Bd\ pL + dl_0\ BpL - dp\ pL\ SHP + d_0\ BpL + lp_1\ L + dl_1\ pBpL + dl_2\ ppBpL + d_1\ pBpL + d_2\ ppBpL$
3. $\frac{d}{dt}BL = r_1\ Bd\ L - dl_0\ BL + dp\ SHP\ pBL + dp\ SHP\ BpL - d_0\ BL - bpa_1\ BL - lp_1\ BL$
4. $\frac{d}{dt}BpL = dp\ SHP\ pBpL - dp\ SHP\ BpL + r_1\ Bd\ pL - dl_0\ BpL - d_0\ BpL - bpa_2\ BpL + lp_1\ BL$
5. $\frac{d}{dt}pBL = -dp\ SHP\ pBL + dp\ SHP\ pBpL - bpa_1\ pBL + bpa_1\ BL + dp\ SHP\ ppBL - lp_1\ pBL - dl_1\ pBL - d_1\ pBL$
6. $\frac{d}{dt}pBpL = -dp\ SHP\ pBpL - dp\ SHP\ pBpL - bpa_2\ pBpL + dp\ SHP\ ppBpL + bpa_2\ BpL + lp_1\ pBL - dl_1\ pBpL - d_1\ pBpL$
7. $\frac{d}{dt}ppBL = bpa_1\ pBL - lp_1\ ppBL - dp\ SHP\ ppBL + dp\ SHP\ ppBpL - dl_2\ ppBL - d_2\ ppBL$
8. $\frac{d}{dt}ppBpL = lp_1\ ppBL + bpa_2\ pBpL - dp\ SHP\ ppBpL - dp\ SHP\ ppBpL - dl_2\ ppBpL - d_2\ ppBpL$
9. $\frac{d}{dt}SHP = sa\ SHPi\ (L + pL) + s'\ SHPi\ (BL + BpL + pBpL + pBL + ppBL + ppBpL) - si\ SHP\ Bd - s\ SHP\ (BL + BpL + pBpL + pBL + ppBL + ppBpL)$

## 2. List of reactions in the model

| S.No | Reaction Name | Reaction | Evidence of reaction | Rate constant |
|---|---|---|---|---|
| 1 | Receptor dimerization | 2 * Bm -> Bd | Harwood et al.[1];Pierce et al.[2];Tolar et al.[3] | $a_1$ |
| 2 | Ligand induced dimerization of receptors | 2 * Bm -> Bd | Harwood et al.[1];Pierce et al.[2];Tolar et al.[3] | $a_2$ |
| 3 | Lyn recruitment to dimerized receptors | Bd + L -> BL | Pleiman et al.[4]; Pierce et al.[2]; Sohn et al.[5, 6] ; Tsourkas et al.[7] | $r_1$ |
| 4 | BCR dimer phosphorylation by Lyn | BL -> pBL | Sotirellis et al.[8] ; Harwood et al.[1]; Kurosaki et al.[9] | $bpa_1$ |
| 5 | Singly phosphorylated BCR dimer phosphorylation by Lyn | pBL -> ppBL | Sotirellis et al.[8] ; Harwood et al.[1]; Kurosaki et al.[9] | $bpa_1$ |
| 6 | Receptor dephosphorylation by SHP | SHP + pBL -> SHP + BL | Veillette et al.[10]; Cyster et al.[11]; Smith et al.[12] | $dp$ |
| 7 | Receptor dephosphorylation by SHP | SHP + ppBL -> SHP + pBL | Veillette et al.[10]; Cyster et al.[11]; Smith et al.[12] | $dp$ |
| 8 | Receptor dimer dissociation into monomers | Bd -> 2 * Bm | Harwood et al.[1];Pierce et al.[2];Tolar et al.[3] | $d$ |
| 9 | Lyn bound dimer dissociation | BL -> 2 * Bm + L | Pierce et al.[2]; Sohn et al.[5, 6]; Tsourkas et al.[7] | $d_0$ |
| 10 | Lyn bound singly phosphorylated dimer Dissociation | pBL -> 2 * Bm + L | Pierce et al.[2]; Sohn et al.[5, 6]; Tsourkas et al.[7] | $d_1$ |
| 11 | Lyn bound doubly phosphorylated dimer dissociation | ppBL -> 2 * Bm + L | Pierce et al.[2]; Sohn et al.[5, 6]; Tsourkas et al.[7] | $d_2$ |
| 12 | Lyn dissociation from unphosphorylated Dimers | BL -> Bd + L | Pleiman et al.[4]; Pierce et al.[2]; Sohn et al.[5, 6] ; Tsourkas et al.[7] | $dl_0$ |
| 13 | Lyn dissociation from singly phosphorylated receptor dimers | pBL -> Bd + L | Pleiman et al.[4]; Tsourkas et al.[7] | $dl_1$ |
| 14 | Lyn dissociation from doubly phosphorylated receptor dimers | ppBL -> Bd + L | Pleiman et al.[4]; Tsourkas et al.[7] | $dl_2$ |
| 15 | SHP activation by Free Lyn | SHPi + L -> SHP + L | Veillette et al.[10]; Smith et al.[12] | $sa$ |
| 16 | SHP inhibition by dimer | SHP + Bd -> SHPi + Bd | Capasso et al.[13] | $si$ |
| 17 | SHP inhibition by Lyn bound receptor | SHP + BL -> SHPi + BL | Capasso et al.[13] | $s$ |

| | | | | |
|---|---|---|---|---|
| 18 | SHP inhibition by Lyn bound receptor | SHP + pBL -> SHPi + pBL | Capasso et al.[13] | $s$ |
| 19 | SHP inhibition by Lyn bound receptor | SHP + ppBL -> SHPi + ppBL | Capasso et al.[13] | $s$ |
| 20 | SHP activation by receptor bound Lyn | SHP + BL -> SHP + BL | Capasso et al.[13] | $s$' |
| 21 | SHP activation by receptor bound Lyn | SHPi + pBL -> SHP + pBL | Capasso et al.[13] | $s$' |
| 22 | SHP activation by receptor bound Lyn | SHPi + ppBL -> SHP + ppBL | Capasso et al.[13] | $s$' |
| 23 | Free Lyn auto-Phosphorylation | L -> pL | Sotirellis et al.[8] | $lp_1$ |
| 24 | Receptor bound Lyn auto-phosphorylation | BL -> BpL | Sotirellis et al.[8] | $lp_1$ |
| 25 | Receptor bound Lyn auto-phosphorylation | pBL -> pBpL | Sotirellis et al.[8] | $lp_1$ |
| 26 | Receptor bound Lyn auto-phosphorylation | ppBL -> ppBpL | Sotirellis et al.[8] | $lp_1$ |
| 27 | Free p-Lyn dephosphorylation by SHP | pL + SHP -> SHP + L | Veillette et al.[10]; Cyster et al.[11]; Smith et al.[12] | $dp$ |
| 28 | Receptor bound Lyn dephosphorylation by SHP | SHP + BpL -> SHP + BL | Veillette et al.[10]; Cyster et al.[11]; Smith et al.[12] | $dp$ |
| 29 | Receptor bound Lyn dephosphorylation by SHP | SHP + pBpL -> SHP + pBL | Veillette et al.[10]; Cyster et al.[11]; Smith et al.[12] | $dp$ |
| 30 | Receptor bound Lyn dephosphorylation by SHP | SHP + ppBpL -> SHP + ppBL | Veillette et al.[10]; Cyster et al.[11]; Smith et al.[12] | $dp$ |
| 31 | p-Lyn recruitment to dimerized receptors | Bd + pL -> BpL | Pleiman et al.[4]; Pierce et al.[2]; Sohn et al.[5, 6] ; Tsourkas et al.[7] | $r_1$ |
| 32 | BCR dimer phosphorylation by p-Lyn | BpL -> pBpL | Sotirellis et al.[8] ; Harwood et al.[1]; Kurosaki et al.[9] | $bpa_2$ |
| 33 | p-BCR dimer phosphorylation by p-Lyn | pBpL -> ppBpL | Sotirellis et al.[8] ; Harwood et al.[1]; Kurosaki et al.[9] | $bpa_2$ |
| 34 | Receptor dephosphorylation by SHP | SHP + pBpL -> SHP + BpL | Veillette et al.[10]; Cyster et al.[11]; Smith et al.[12] | $dp$ |
| 35 | Receptor dephosphorylation by SHP | SHP + ppBpL -> SHP + pBpL | Veillette et al.[10]; Cyster et al.[11]; Smith et al.[12] | $dp$ |
| 36 | p-Lyn bound dimer dissociation | BpL -> 2 * Bm + pL | Pierce et al.[2]; Sohn et al.[5, 6]; Tsourkas et al.[7] | $d_0$ |
| 37 | p-Lyn bound singly phosphorylated dimer dissociation | pBpL -> 2 * Bm + pL | Pierce et al.[2]; Sohn et al.[5, 6]; Tsourkas et al.[7] | $d_1$ |
| 38 | p-Lyn bound doubly phosphorylated dimer dissociation | ppBpL -> 2 * Bm + L | Pierce et al.[2]; Sohn et al.[5, 6]; Tsourkas et al.[7] | $d_2$ |

| | | | | |
|---|---|---|---|---|
| 39 | p-Lyn dissociation from unphosphorylated dimers | BpL -> Bd + pL | Pleiman et al.[4]; Pierce et al.[2]; Sohn et al.[5, 6] ; Tsourkas et al.[7] | $dl_0$ |
| 40 | p-Lyn dissociation from singly phosphorylated receptor dimers | pBpL -> Bd + pL | Pleiman et al.[4]; Tsourkas et al.[7] | $dl_1$ |
| 41 | p-Lyn dissociation from doubly phosphorylated receptor dimers | ppBpL -> Bd + pL | Pleiman et al.[4]; Tsourkas et al.[7] | $dl_2$ |
| 42 | SHP activation by Free p-Lyn | SHPi + pL -> SHP + pL | Veillette et al.[10]; Smith et al.[12] | *sa* |
| 43 | SHP inhibition by Lyn bound receptor | SHP + BpL -> SHPi + BpL | Capasso et al.[13] | *s* |
| 44 | SHP inhibition by Lyn bound receptor | SHP + pBpL -> SHPi + pBpL | Capasso et al.[13] | *s* |
| 45 | SHP inhibition by Lyn bound receptor | SHP + ppBpL -> SHPi + ppBpL | Capasso et al.[13] | *s* |
| 46 | SHP activation by receptor bound Lyn | SHPi + BpL -> SHP + BpL | Capasso et al.[13] | *s*’ |
| 47 | SHP activation by receptor bound Lyn | SHPi + pBpL -> SHP + pBpL | Capasso et al.[13] | *s*’ |
| 48 | SHP activation by receptor bound Lyn | SHPi + ppBpL -> SHP + ppBpL | Capasso et al.[13] | *s*’ |

## 3. Fixing the reference set of parameters in the model

**Evidence for parameters from the literature** (*first section of Table 1*)

The parameters used in our model are listed in Table 1 of the main text. We have segregated the parameters into three groups depending on the literature evidence. As shown in the Table 1 the first section corresponds to the parameters that were directly available from earlier experimental/modeling studies. We obtained the values of Lyn recruitment $r_1$, dissociation parameter $dl_0$ and phosphorylation parameter $bpa_1$ from the FceRI signaling model[14, 15] due to the similarity between FceRI and BCR signaling. Receptor phosphorylation mediated by phosphorylated Lyn ($bpa_2$) was taken to be 10 times greater than that mediated by unphosphorylated Lyn ($bpa_1$) since it is known that the catalytic activity of Lyn increases ~17 fold upon its phosphorylation.[8] The total number of Lyn molecules (*Lt*) is known to be limiting in lymphocytes[15, 16] and literature values suggest *Lt* to be ~25000 molecules.[14, 15] The total number of SHP molecules (*St* ~$10^5$) and BCRs (*Bt*~$10^5$) were also obtained from literature.[17,18]

*Evidence for dephosphorylation parameter (dp)*

Dephosphorylation of both receptors and Lyn molecules are mediated by SHP. In our model we have included SHP regulation via a second order term (eg. $d[pBL]/dt = -dp\ [pBL]\ [SHP]$ + *other terms*). The dephosphorylation parameter *dp* has dimensions molecule$^{-1}$sec$^{-1}$. In a Michaelis Menten scheme the *dp* value is given by $k_{cat}/K_m$ which denotes the catalytic efficiency of the phosphatase SHP1. Experimental measurements of SHP1 catalytic efficiency $k_{cat}/K_m$ ($\approx dp$) for pY peptides range from 0.002 to 23 $\mu M^{-1}s^{-1}$.[19] We were interested in SHP1 dephosphorylation of BCR ITAMs and Lyn for which precise experimental evidence was not available. However $k_{cat}/K_m$ values for a peptide sequence optimally representing a src substrate (Lyn belongs to src family of kinases) was found to be 5.63 $\mu M^{-1}s^{-1}$.[20] This value of $k_{cat}/K_m$ corresponds to $dp \sim 0.7\times10^{-4}$ molecule$^{-1}$sec$^{-1}$, where the volume of a B cell has been taken to be ~135 $\mu m^3$ ($1.35\times10^{-13}$ *l*) consistent with the known literature on average B cell dimensions.[21] Based on this we took the reference value of *dp* in the model to be $10^{-4}$ molecule$^{-1}s^{-1}$ (Table 1). As an independent check, we note that generally in the literature the dephosphorylation reaction is considered to be a pseudo first-order reaction (eg. $d[pBL]/dt = -dp'\ [pBL]$ + *other terms*) and the value of *dp'* ranges between 1-100 sec$^{-1}$.[14, 22] Comparing with the second order term used in the present model it follows that $dp' = dp[SHP]_{ss}$. Where $[SHP]_{ss}$ denotes steady state concentration of SHP. In our simulations we found that in the ON steady state the value of SHP was found ~ 65000 molecules. Thus *dp* [SHP] in this state ~ 6.5 $s^{-1}$ which is well within the range of *dp*' values 1-100$s^{-1}$ found in the literature. [14, 22] In our model for simplicity we consider the rate of dephosphorylation by SHP (*dp*) to be the same for BCR ITAMs as well as free and bound forms of Lyn. We also studied the behaviour of the model for a range of values of *dp*, keeping the other parameters fixed. We

determined the range of values of *dp* for which the model exhibits bistability. Figure S5 shows that the model tolerates more than a 15 fold increase and ~ 2 fold decrease around the reference value while still exhibiting bistability.

*Parameters in the second section of Table 1*

The second section in Table 1 lists the parameters that could not be obtained directly from literature but whose values can be constrained by existing experimental evidence. Constraints can be of two types. In the first type, experiments suggest that a function of some variables has a specific value (this limits parameter freedom to a lower dimensional hypersurface of parameter space). The second type of constraint is an upper or lower bound on (some function of) the parameters. Below we discuss the estimation of such parameters from the available literature and modeling considerations. Parameters for spontaneous receptor dimerization ($a_1$) and dissociation ($d$) are not easy to measure experimentally. But in the absence of ligand it is known that ~20-30 % of the BCRs exist as dimers or higher order oligomers.[23] Since literature values of total number of BCR in B cells is ~100000,[18] under steady state conditions therefore ~70000-80000 receptor molecules would exist in monomeric form and the rest would form dimers. We could then constrain $a_1$ and $d$ as follows. Assuming for simplicity that in the tonic state the only relevant processes are the spontaneous dimerization of the receptors and their dissociation into monomers, we have $\frac{d[Bd]}{dt} = a_1[Bm]^2 - d[Bd]$, where, [Bd]=Number of BCR dimers, [Bm]=Number of BCR monomers. Under steady state conditions, this implies

$$a_1[Bm]^2 - d[Bd] = 0.$$

From the above condition it can be seen that the ratio $d/a_1$ of the dimer dissociation rate $d$ and the spontaneous dimerization rate $a_1$ is constrained by the experimental fact that ~20-30% of BCRs exist as dimers or higher order oligomers. Using [Bm]=(0.7-0.8)×Bt, [Bd]=(1/2) [Bt-Bm], Bt=$10^5$ we get $d/a_1$ in the range (3.3-6.4)×$10^5$. We work with a default value of $d/a_1 = 5\times10^5$.

In order to get an estimate of $a_1$ and $d$ any one of these rate constants must be fixed appropriately and the other rate constant can then be identified. An approximate range of spontaneous receptor clustering can be considered to be ≤ the aggregation rate due to ligand. Earlier studies on FcεRI signaling estimated the ligand induced aggregation rate to be ~$10^{-2}$ molecule$^{-1}$sec$^{-1}$.[15] By assuming $a_1$ to be 0.001 molecule$^{-1}$sec$^{-1}$, $d$ can be estimated to be 500 sec$^{-1}$, which we have employed as our reference value in the model (see Table 1). We also investigated the model for a range of $a_1$ and $d$ values (respectively 7 and 4 orders of magnitude around the reference value); the resulting phase diagram is shown in Figure S1. It is evident that bistability exists in a substantial region of parameter space and hence is a robust property of the model. The red line corresponds to

traversing the $a_1$-$d$ parameter space under the constraint $d/a_1=5\times10^5$. This line cuts both the phase boundaries of the bistable region; hence it is in principle possible to be in any of the 3 phases while preserving the experimental constraint represented by this line. This analysis strengthens our parameter estimates and highlights the robustness of the model for the changes in $a_1$ and $d$. Moreover we determined the behaviour of the model for independent variations in $dp$ and $a_1$ (or $d$) keeping $d/a1$ fixed at $5\times10^5$. Figure S2 shows the ranges of bistability for varying $dp$, $a_1$ and $d$ values. One can clearly see the substantial range of bistability in the model.

We assumed the Lyn auto phosphorylation rate $lp_1$ to be the same as $bpa_1$, the rate constant for the phosphorylation of BCR by Lyn, i.e., 10 $sec^{-1}$. The model is very robust to changes in both these parameters. For example the bistability continues to exist if any of them is individually varied by more than 2 orders of magnitude in either direction (Fig. S5). Parameters regulating the dissociation of Lyn from singly and doubly phosphorylated BCR dimers $dl_1$ and $dl_2$ are not known experimentally. However, it is known that upon phosphorylation of the α subunit of BCR ITAM, Lyn recruitment to it is enhanced several folds[4, 23] suggesting that BCR phosphorylation stabilizes BCR-Lyn complex i.e., $dl_1$ and $dl_2$ are much smaller than $dl_0$. Since precise parameter values for the slower dissociation of Lyn from the phosphorylated BCR-Lyn complexes are not known we varied $dl_1$ and $dl_2$ over a several orders of magnitude and determined the behaviour of the model (Fig. S4). The figure shows that for any fixed value of $r_1$, the system shows bistability when $dl_1$ and $dl_2$ are small enough. As reference values for the model we chose $dl_1=10^{-3}s^{-1}$ and $dl_2=10^{-6}s^{-1}$, thereby placing the model well inside the bistable region of the phase diagram. Note that these values of $dl_1$ and $dl_2$ are smaller than $dl_0$. Figure S4 also shows that the region of bistability can be extended for larger values of $r_1$, the Lyn recruitment parameter. For example, with $r_1=10^{-4}$ (twice our reference value), bistability would still exist at $dl_1=0.1s^{-1}$, $dl_2=10^{-3}s^{-1}$. However beyond a certain value of $r_1$ bistability is lost; see Panel B in Figure S4. The dependence of the phase structure on $r_1$ and $dl_2$ is shown in more detail in Panel B of Figure S4. The $dl_0$ dependence of the phase boundaries in the $dl_1$-$dl_2$ plane is shown in Figure S9 Panel B. Collectively this analysis shows that $dl_1$ and $dl_2$ should be significantly smaller than $dl_0$ for the bistability to exist in the model, i.e., phosphorylation should enhance the stability of the BCR-Lyn complex significantly. We note that requirement of $dl_1$ and $dl_2$ to be small is less stringent in the trimer model than it is in the dimer model. (Fig. S7)

*Parameters in the third section of Table 1*

The third section has parameters relating to dissociation of various dimer species into monomers as well as those relating to regulation of SHP activity, which are at present experimentally undetermined to our knowledge. These include the activation of SHP by Lyn (*sa*) which is in fact mediated by CD22 and the inhibition of SHP by plain BCR dimers (*si*) which is mediated by ROS. Since experimental evidence was not available we assumed *sa* and *si*

to be free parameters in the model. We performed 2D parameter-space bifurcation analysis of *sa* vs *si* (keeping *s*=*si*) so that the robustness of the model with respect to these parameters can be seen (Fig. S3). The system showed a very large range of bistability. As with $dl_1$ and $dl_2$ the reference values of parameters were also fixed to place the model in the bistable region as shown in the Figure S3. As evident from Figure S3 if both *sa* and *si* are increased or decreased together, bistability is preserved over several orders of magnitude. It is not known whether the complexes of BCR dimers with Lyn activate or inhibit SHP. In our reference set of parameters we assumed that they inhibit SHP (case (1) discussed in the main text) with the same rate as plain dimers (*s*=*si*) for simplicity. Therefore *s*' was set equal to zero under case (1).

The dissociation rate of plain dimers into monomers is *d*, and its fixation was discussed earlier. Literature evidence suggests that phosphorylated dimers dissociate into monomers at much slower rates than unphosphorylated dimers [23, 24]. Therefore we assumed that $d_0 = d$ and $d_1 = d_2 = 0$ for the base dimer model. The case ($d_1$=) $d_2 \leq d$ (=$d_0$) was considered separately and is described in Figure S9A.

## 4. Procedure for studying the effect of removal of links 2, 3 and 8 in the model

The effect of removal of links 2, 3 and 8 was studied in a simplified model in which phosphorylated Lyn and all its associated complexes are excluded.

*List of reactions of the simplified model*

1. 2 * Bm -> Bd
2. Bd + L -> BL
3. BL -> pBL
4. pBL -> ppBL
5. SHP + pBL -> SHP + BL
6. SHP + ppBL -> SHP + pBL
7. Bd -> 2 * Bm
8. BL -> 2 * Bm + L
9. pBL -> 2 * Bm + L
10. ppBL -> 2 * Bm + L
11. BL -> Bd + L
12. pBL -> Bd + L
13. ppBL -> Bd + L
14. SHPi + L -> SHP + L
15. SHP + Bd -> SHPi + Bd
16. SHP + BL -> SHPi + BL
17. SHP + pBL -> SHPi + pBL
18. SHP + ppBL -> SHPi + ppBL

The ODE model using mass action kinetics with the above set of reactions exhibits bistability as expected, since all the links given in Figure 6A are intact for this simplified model. We analyzed this model and its variants (corresponding to removal of links 2, 3 and 8) using the Chemical Reaction Network Theory (CRNT). The toolbox for CRNT accepts the mass action reactions as input and analyzes the topology of the model to identify existence of multiple steady states in the system. Complete details of CRNT can be found in Feinberg et al.[25,26] Using assumptions detailed below we obtained variants of this model by removing the particular links.

1. ***Removal of link 2:*** This was achieved by considering SHP activation to be spontaneous and not dependent on any form of Lyn, i.e., SHP activation happens spontaneously at a constant rate. This implies that the dynamics of Lyn and its recruitment to the receptor dimers does not have any effect on SHP activation. However SHP inhibition still depends on *si* and the amount of plain BCR dimers (Bd). Thus the reaction **No. 14 SHPi + L -> SHP + L** is changed to **SHPi -> SHP** while the remaining reactions are kept the same. This assumption in our model causes the removal of link 2 while preserving the other links. The model with link 2 removed in this fashion was analyzed using CRNT. It was found that this model was capable of supporting bistability in some region of its parameter space.

2. ***Removal of link 3:*** Link 3 can be removed by assuming receptor dimer dephosphorylation to be a spontaneous decay independent of SHP. Then SHP activation status does not influence dimer dephosphorylation leading to loss of three feedbacks. Reactions **5: SHP + pBL -> SHP + BL** and **6: SHP + ppBL -> SHP + pBL** are respectively converted to **pBL -> BL** and **ppBL ->pBL**. The perturbed model did not exhibit bistability any where in its parameter space.

3. ***Removal of link 8:*** This is achieved by considering conversion of active SHP to inactive SHP to be spontaneous and independent of any form of BCR dimers. i.e., reactions **15-18: SHP + Bd -> SHPi + Bd, SHP + BL -> SHPi + BL, SHP + pBL -> SHPi + pBL, SHP + ppBL -> SHPi + ppBL** are replaced by the single reaction **SHP -> SHPi.** This model displays bistability in some region of its parameter space. However when links 2 and 8 are removed simultaneously (i.e., the perturbations listed in (1) and (3) are made together), the resulting model does not show bistability anywhere in the parameter space.

## 5. References


1. N. E. Harwood and F. D. Batista, *Annu Rev Immunol*, 2010, **28**, 185-210.
2. S. K. Pierce and W. Liu, *Nat Rev Immunol*, 2010, **10**, 767-777.
3. P. Tolar, J. Hanna, P. D. Krueger and S. K. Pierce, *Immunity*, 2009, **30**, 44-55.
4. C. M. Pleiman, C. Abrams, L. T. Gauen, W. Bedzyk, J. Jongstra, A. S. Shaw and J. C. Cambier, *Proc Natl Acad Sci U S A*, 1994, **91**, 4268-4272.
5. H. W. Sohn, P. Tolar and S. K. Pierce, *J Cell Biol*, 2008, **182**, 367-379.
6. H. W. Sohn, P. Tolar, T. Jin and S. K. Pierce, *Proc Natl Acad Sci U S A*, 2006, **103**, 8143-8148.
7. P. K. Tsourkas, W. Liu, S. C. Das, S. K. Pierce and S. Raychaudhuri, *Cell Mol Immunol*, 2012, **9**, 62-74.
8. N. Sotirellis, T. M. Johnson, M. L. Hibbs, I. J. Stanley, E. Stanley, A. R. Dunn and H. C. Cheng, *J Biol Chem*, 1995, **270**, 29773-29780.
9. T. Kurosaki, *Annu Rev Immunol*, 1999, **17**, 555-592.
10. A. Veillette, S. Latour and D. Davidson, *Annu Rev Immunol*, 2002, **20**, 669-707.
11. J. G. Cyster and C. C. Goodnow, *Immunity*, 1995, **2**, 13-24.
12. K. G. Smith, D. M. Tarlinton, G. M. Doody, M. L. Hibbs and D. T. Fearon, *J Exp Med*, 1998, **187**, 807-811.
13. M. Capasso, M. K. Bhamrah, T. Henley, R. S. Boyd, C. Langlais, K. Cain, D. Dinsdale, K. Pulford, M. Khan, B. Musset, V. V. Cherny, D. Morgan, R. D. Gascoyne, E. Vigorito, T. E. DeCoursey, I. C. MacLennan and M. J. Dyer, *Nat Immunol*, 2010, **11**, 265-272.
14. J. R. Faeder, W. S. Hlavacek, I. Reischl, M. L. Blinov, H. Metzger, A. Redondo, C. Wofsy and B. Goldstein, *J Immunol*, 2003, **170**, 3769-3781.
15. C. Wofsy, C. Torigoe, U. M. Kent, H. Metzger and B. Goldstein, *J Immunol*, 1997, **159**, 5984-5992.
16. B. Goldstein, J. R. Faeder and W. S. Hlavacek, *Nat Rev Immunol*, 2004, **4**, 445-456.
17. V. Raia, M. Schilling, M. Bohm, B. Hahn, A. Kowarsch, A. Raue, C. Sticht, S. Bohl, M. Saile, P. Moller, N. Gretz, J. Timmer, F. Theis, W. D. Lehmann, P. Lichter and U. Klingmuller, *Cancer Res*, 2011, **71**, 693-704.
18. G. I. Bell, *Immunology today*, 1983, **4**, 237-240.
19. L. Ren, X. Chen, R. Luechapanichkul, N. G. Selner, T. M. Meyer, A. S. Wavreille, R. Chan, C. Iorio, X. Zhou, B. G. Neel and D. Pei, *Biochemistry*, 2011, **50**, 2339-2356.
20. C. Frank, C. Burkhardt, D. Imhof, J. Ringel, O. Zschornig, K. Wieligmann, M. Zacharias and F. D. Bohmer, *J Biol Chem*, 2004, **279**, 11375-11383.
21. C. B. Thompson, I. Scher, M. E. Schaefer, T. Lindsten, F. D. Finkelman and J. J. Mond, *J Immunol*, 1984, **133**, 2333-2342.
22. B. Hat, B. Kazmierczak and T. Lipniacki, *PLoS Comput Biol*, 2011, **7**, e1002197.
23. P. Tolar, H. W. Sohn and S. K. Pierce, *Nat Immunol*, 2005, **6**, 1168-1176.
24. A. Kulczycki, Jr. and H. Metzger, *J Exp Med*, 1974, **140**, 1676-1695.
25. M. Feinberg, *Arch Rational Mech Anal*, 1995, **132**, 311-370.
26. M. Feinberg, *http://www.chbmeng.ohio-state.edu/~feinberg/crnt/*.

# 6 Supplementary Figures

Figure S1

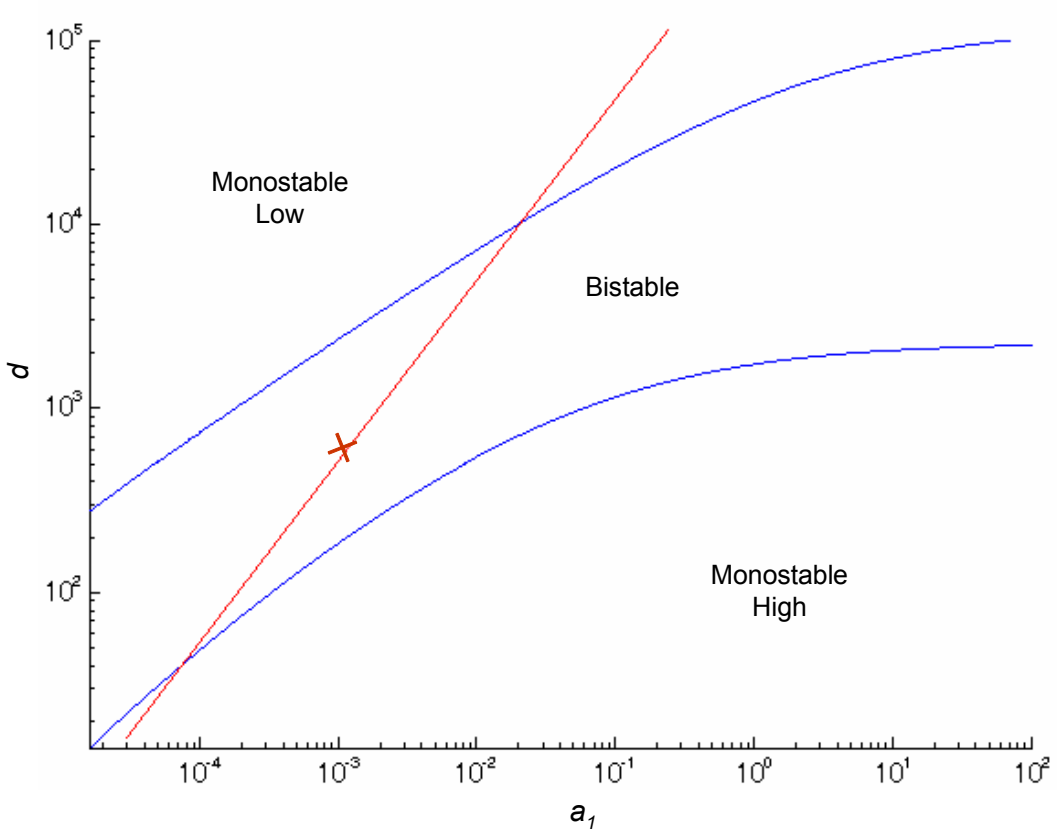


**Robustness of the bistability in the model with respect to changes in $a_1$ and $d$**
The figure shows the 2D parameter space diagram of $a_1$ and $d$. Other parameters are as in Table 1. The red line indicates the constraint $d/a_1=5\times10^5$, while the red cross indicates the default parameter value for $a_1$ and $d$ in our model simulations. It is evident that the bistability persists in the model for a substantial region of parameter space around the reference value. At the same time, ligand induced receptor clustering, which effectively increases the $a_1$ parameter and/or decreases the $d$ parameter can cause the system to enter the monostable high phase and exhibit the switch like behaviour discussed in the main text.

Figure S2

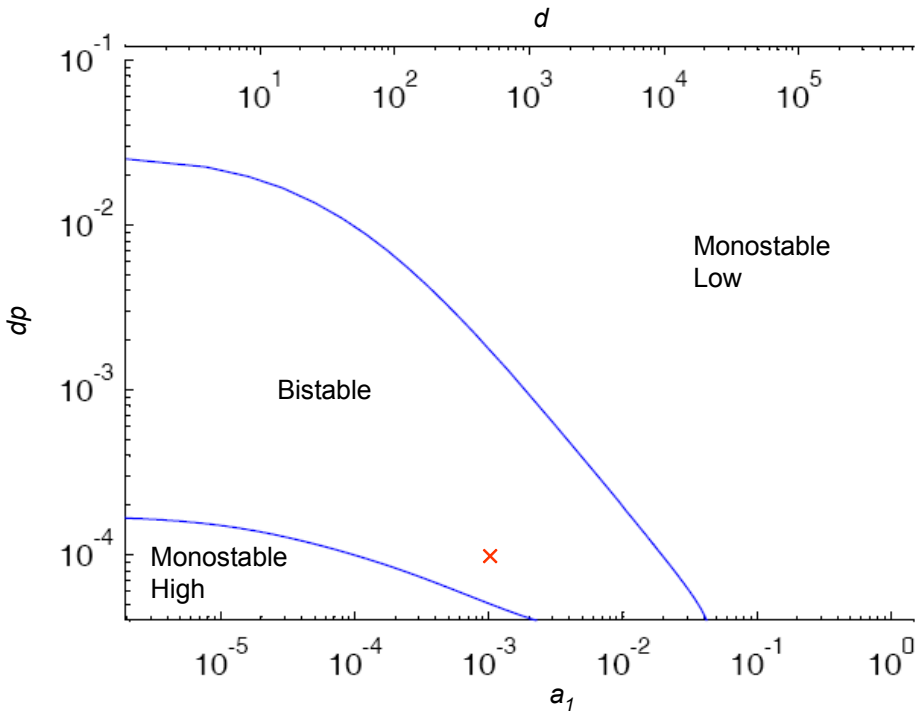


**Robustness of bistability in the model with respect to changes in $a_1$, $d$ and $dp$**
The figure shows the 2D parameter diagram for $a_1$ (or $d$) and $dp$. ($a_1$ and $d$ are varied keeping $d/a_1=5\times10^5$, see discussion under 'Fixing the reference set of parameter values' in supplementary text). Regions of bistability and monostability are appropriately marked. A large range of bistability can be seen for $dp$ for a given value of $a_1$ and $d$ indicating the robustness of qualitative output of the model for the parameter changes. The red cross indicates the reference value of the parameters in the model.

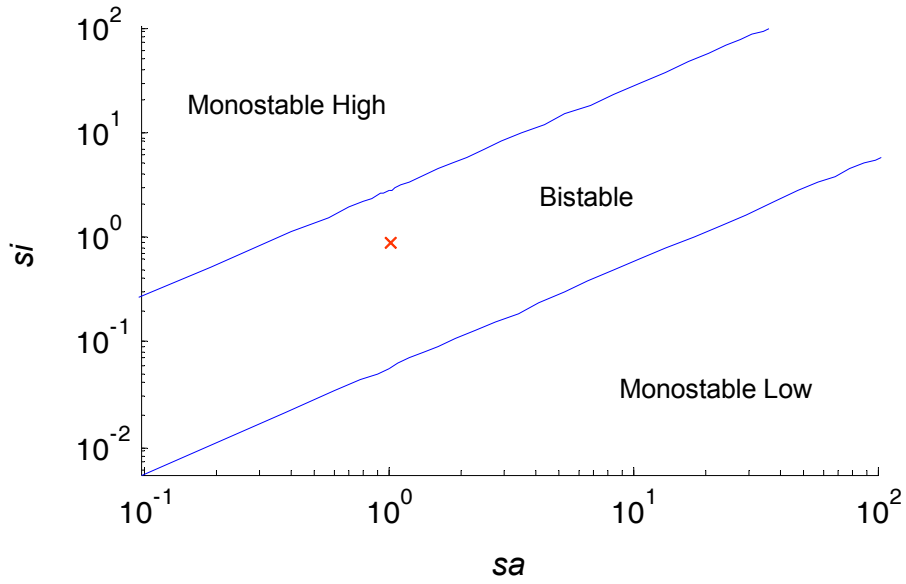


**Robustness of bistability in the model with respect to changes in *sa* and *si***
The figure shows the 2D parameter-space diagram for *sa* and *si* parameters while keeping *s*=*si*. The red cross indicates the reference value of the parameters in our model. It is evident that bistability is robust with respect to variations in these parameters, especially if these parameters are varied together.

Figure S4




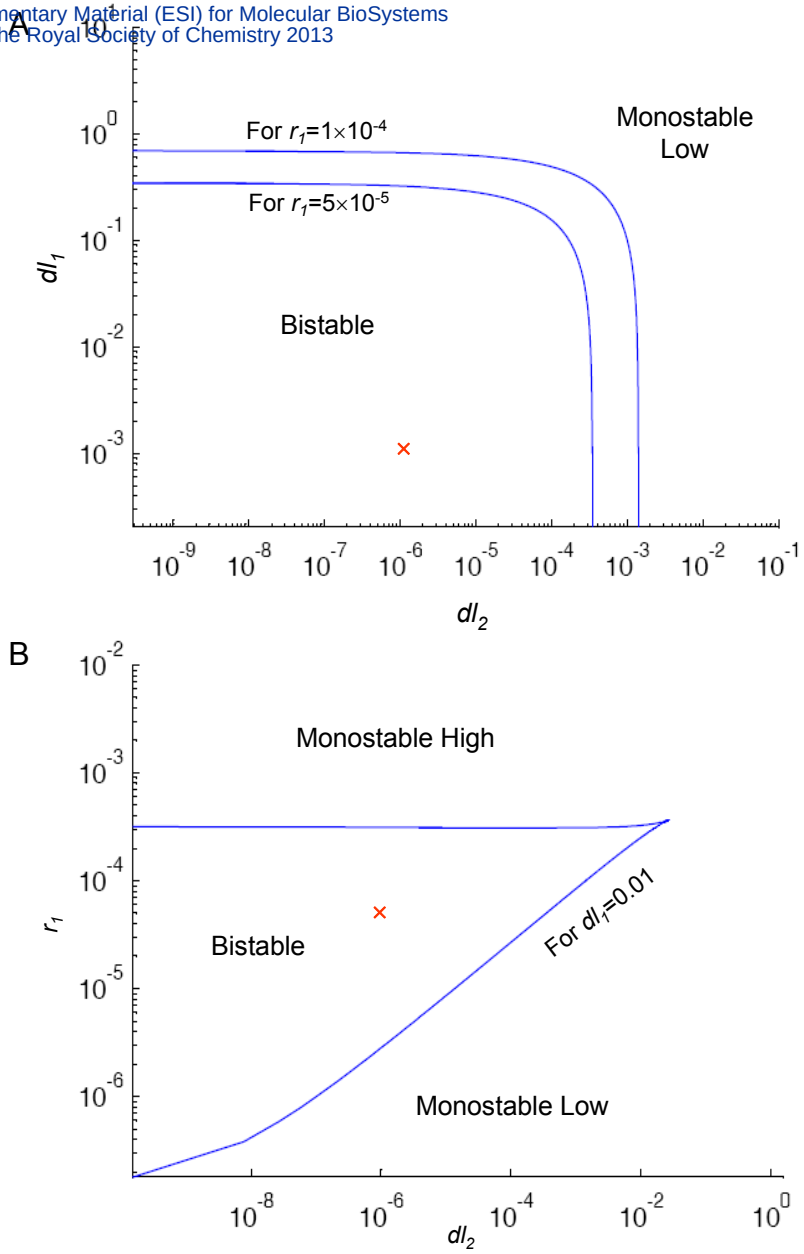


**Robustness of the bistability in the model with respect to changes in $dl_1$, $dl_2$ and $r_1$**

Panel A shows the 2D parameter space diagram of $dl_1$ and $dl_2$ for different values of $r_1$. It can be seen that there is a substantial range of parameters for which bistability exists. It is evident that as $r_1$ is increased the region of $dl_1$-$dl_2$ phase where bistability exist expands. Bistability can exist for values of $dl_2$ as high as $10^{-3}$ when $r_1$ is increased from $5 \times 10^{-5}$ to $1 \times 10^{-4}$. The red cross indicates the reference value of the parameters in our model.

Panel B shows the 2D parameter space diagram of $dl_2$ and $r_1$ for a fixed value of $dl_1$ (=0.01) which is greater than the default value in Table 1. It can be seen that as $r_1$ is increased by one order of magnitude (for example from $10^{-5}$ to $10^{-4}$) the upper limit of $dl_2$ where bistability exists increases by at least by two orders of magnitude (i.e., from $10^{-5}$ to $10^{-3}$)

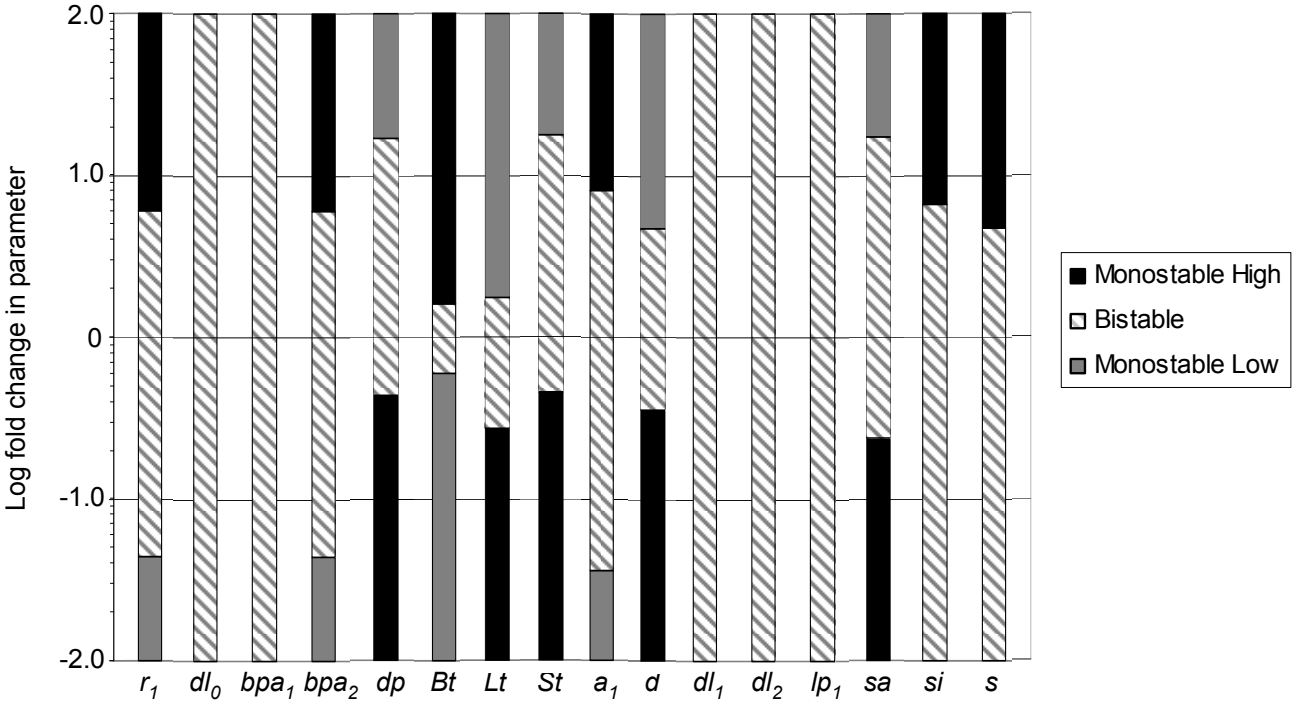


**Parameter robustness analysis**.
The figure shows the ranges of bistability with respect to all the parameters in the dimer model. The value of each parameter was varied individually 100 fold (two orders of magnitude) above and below the reference value listed in Table 1. The parameter varied is given in the x-axis, and the default value of the parameter under study corresponds to zero on the y-axis. A value of 2 on the y-axis corresponds to a 100 fold increase from the reference value. The parameter range in which the model exhibits bistability is shown by stripes.

Figure S6.

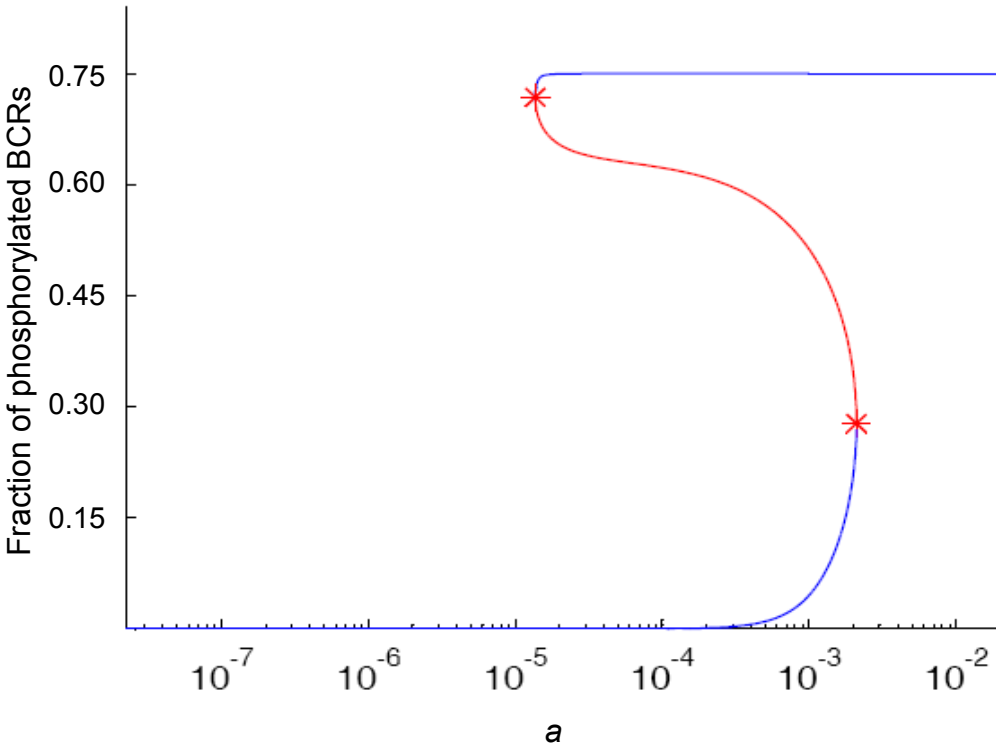


**Bistability in the trimer model**

Figure S6 is the bifurcation diagram showing the fraction of phosphorylated BCR versus $a_2$ for the trimer model. Parameters employed are the same as in Table 1. The additional parameter $dl_3$ has been taken to be equal to $dl_2$. The red stars indicate the two saddle node bifurcation points where the system switches from stable to unstable state and vice versa. The red curve between the two saddle nodes represents unstable steady states and the blue curves denotes the stable steady states. In the x-axis $a \equiv (a_1+a_2)$ is plotted to show both the bifurcation points clearly. It is evident that the fold increase in the receptor activity (y-axis) between the two bifurcation points (red stars) is greater in the trimer case compared to the dimer (see Figure 3B in main text). Also the increase in receptor activity occurs at a lower value of $a$ and is more steep, compared to the dimer model (Fig. 3B).

Figure S7

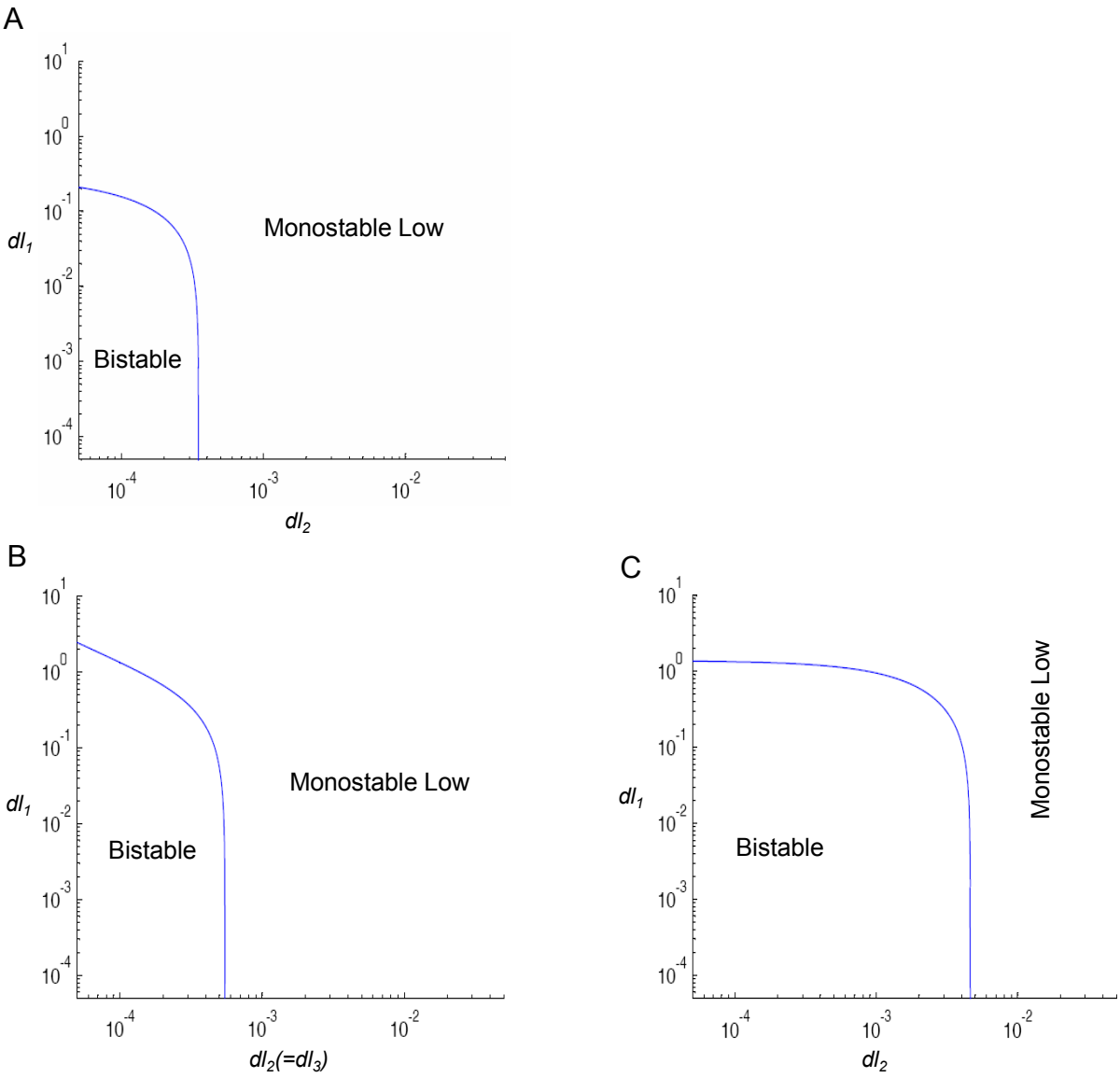


**Enhanced robustness of bistability in the trimer model**

Figure S7 shows the 2D parameter space diagrams of $dI_1$ and $dI_2$ for comparing the dimer model (S7A) and the trimer model (S7B and S7C). In all three panels the parameters of both models except $dI_1$ and $dI_2$ are the same as in Table 1. In Panel B $dI_3$ has been chosen to be equal to $dI_2$, and in Panel C $dI_3$ is fixed at $10^{-4}$.

In the dimer model bistability requires that the rates of Lyn dissociation from phosphorylated dimers ($dI_1$ and $dI_2$) be restricted to the 'bistable region' shown in Panel A.

Panel B and C show that the trimer model has a larger bistable region and hence more robust. In particular the values of the Lyn dissociation rates from phosphorylated receptors do not have to be as small in the trimer model as they have to be in the dimer model.

Figure S8

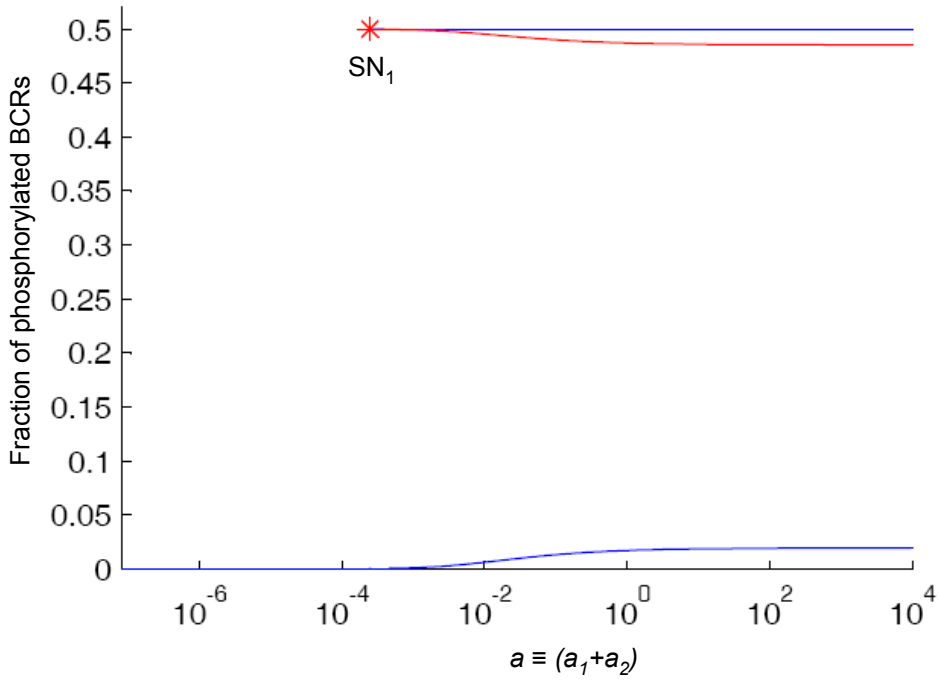


**Effect of ligand induced clustering in presence of high phosphatase activity *dp***
The figure shows the bifurcation diagram of *a* with respect to phosphorylated fraction of the receptors. Here the value of *dp* was fixed at 0.0005,which is larger than the value 0.0001 in the Table 1 while the remaining parameters were the same as in Table 1. Comparing with Fig 3B of the main text, where the same qualities are plotted but at *dp*=0.0001, we see that while the saddle node bifurcation point $SN_1$ exists, the point $SN_2$ has been pushed out. Therefore with an increase of $a_2$ caused by ligand binding the system does not exhibit the switching from low activity state to high activity state.

Figure S9

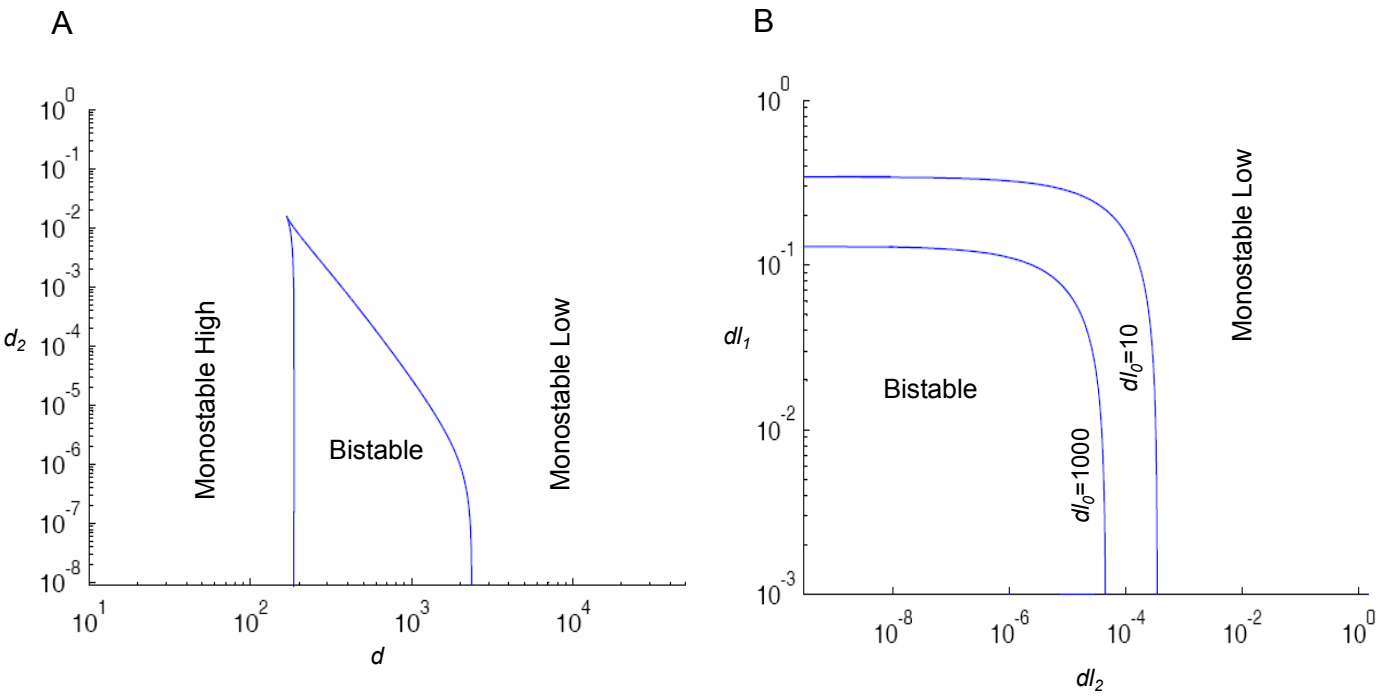


**Effects of changing the strengths of links 4 and 7 on the phase structure of the model**

Panel A shows the 2D parameter space diagram of $d$ and $d_2$. Other parameters take the default values given in Table 1 of the main text. It can be seen that bistability exists only when $d_2$ is smaller than $d$ by several orders of magnitude, implying that link 4 (in Fig 6A of main text). should be sufficiently strong for system bistability.

Panel B shows the 2D parameter space diagram of $dl_1$ and $dl_2$ for different values of $dl_0$. It can be seen that bistability exists only when $dl_1$ and $dl_2$ are significantly smaller than $dl_0$ (for default values of the other parameters), implying that link 7 (in Fig. 6A of main text) should be sufficiently strong for system bistability.

Figure S10

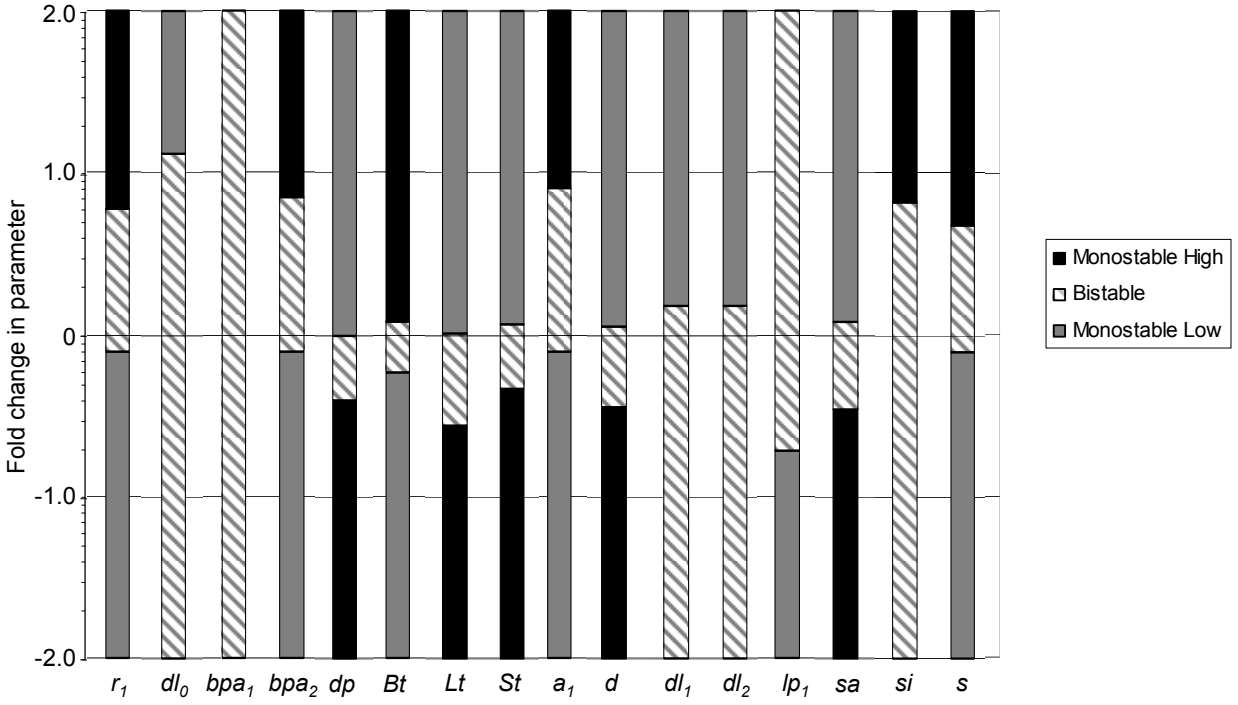


**Parameter robustness analysis of the model after weakening of the positive feedbacks contributed by link 7.**

The plot shows the ranges of bistability with respect to all parameters in the model with $dl_1$=0.1 molecule$^{-1}$sec$^{-1}$ and $dl_2$=10$^{-4}$ molecule$^{-1}$sec$^{-1}$ the remaining parameters were same as the default values in Table 1. The plot was generated as in Figure S5. It can be seen that increasing the values of $dl_1$ and $dl_2$ from those given in Table 1 to present values (hence weakening the link 7 and feedbacks 2-3-7 and 6-7) leads to much reduced region of bistability in the system compared to Figure S5.

Electronic Supplementary Material (ESI) for Molecular BioSystems


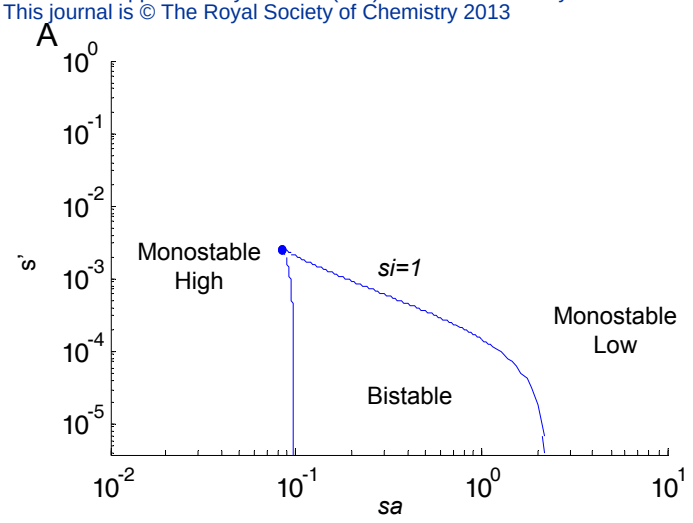


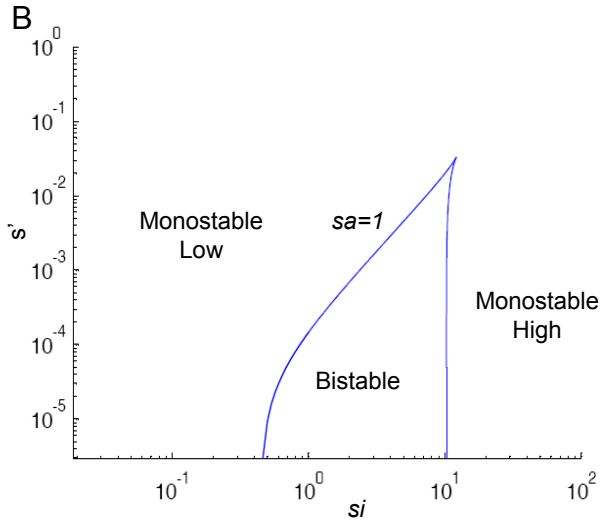


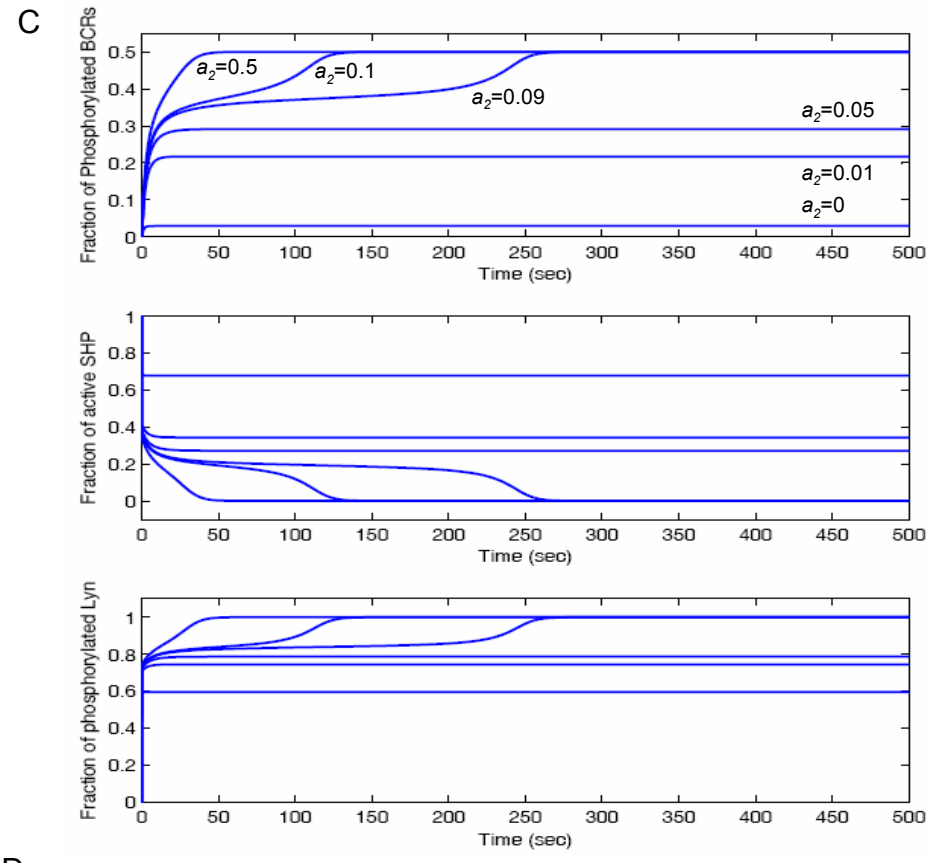


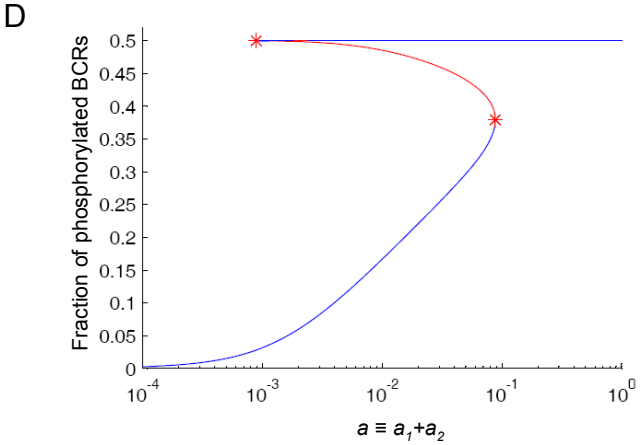

**Results of model simulation with Case (2)**

Here we show simulations of the model under the assumption that Lyn bound BCR dimer Complexes activate SHP rather than inhibit it. Thus we take $s'>0$ and $s=0$. All other parameters Take their reference value as in Table 1, except $s'$, $sa$ and $si$ which also vary in the Panels A and B

Panel A is the bifurcation analysis of $s'$ vs $sa$ with $si$ fixed to unity. Panel B is similar except that it shows bifurcation of $s'$ vs $si$ with $sa=1$.

Panel C shows time course simulations of three quantities of the model namely, phosphorylated BCR, phosphorylated Lyn and active SHP as a fraction of their total concentrations for increasing values of ligand induced clustering parameter $a_2$. The parameters are as in Table 1, except $s=0$ and $s'=10^{-4}$. Here, initial conditions for the fractions of the monomeric BCRs, active SHP and free Lyn were taken to be unity (i.e. Bm=$Bt$, SHP=$St$ and L=$Lt$) and the remaining variables (including all forms of dimers and Lyn bound dimers) were kept at zero.

Panel D shows the bifurcation diagram of $a$ ($\equiv a_1+a_2$) versus phosphorylated fraction of BCR. All other parameters are as in Panel C. The figure illustrates the input threshold dependent bistable switch. The blue lines represent stable steady states; the red line represents an unstable steady state. The red dots indicate the two saddle node bifurcation points where the system switches from stable to unstable state and vice versa.

Electronic Supplementary Material (ESI) for Molecular BioSystems


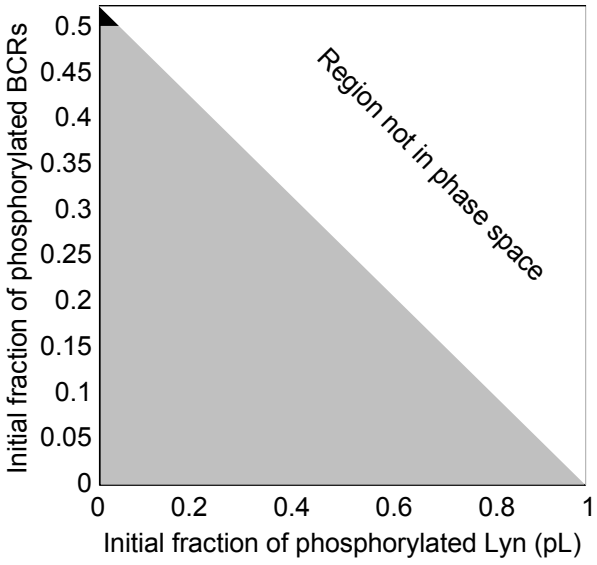


**Projection of the attractor basins of the two steady states on the ppBpL-pL plane.**
In the set of initial conditions considered here, ppBpL and pL are varied, while Bd, BL, BpL, pBL, pBpL, ppBL and SHPi are zero. The initial conditions of L, SHP and Bm are determined by the constraint equations of total protein numbers.
The figure shows the basin sizes of the two steady states. The grey region corresponds to the 'tonic' basin or attractor where initial conditions of the fraction of phosphorylated BCR (ppBpL) and phosphorylated Lyn (pL) lead to the tonic state of the system. The black region corresponds to the 'ON' basin of the B cells. The relative sizes of the basins can be observed from the figure. It must be noted that the empty white region does not exist in the phase space of the system because of the constraint [ppBpL=*Lt*-(L+pL+BL+pBL+ppBL+pBpL)] and the requirement that all concentrations are non-negative.